Correlation between crystal structure and magnetism in the frustrated antiferromagnet $CuFeO_2$ under high magnetic fields

N. Terada,[1,*] Y. Narumi,[2] Y. Sawai,[3] K. Katsumata,[1] U. Staub,[4] Y. Tanaka,[1] A. Kikkawa,[1] T. Fukui,[2] K. Kindo,[2] T. Yamamoto,[3] R. Kanmuri,[3] M. Hagiwara,[3] H. Toyokawa,[5] T. Ishikawa,[1] and H. Kitamura[1]

[1]*RIKEN SPring-8 Center, Harima Institute, Sayo, Hyogo 679-5148, Japan*

[2]*ISSP, University of Tokyo, Kashiwa, Chiba 277-8581, Japan*

[3]*KYOKUGEN, Osaka University, Toyonaka, Osaka 560-8531, Japan*

[4]*Swiss Light Source, Paul Scherrer Institut, 5232 Villigen, Switzerland*

[5]*SPring/JASRI, Sayo, Hyogo 679-5198, Japan*

(Received 7 March 2007; published 11 June 2007)

The results of synchrotron x-ray-diffraction and magnetization measurements on a triangular lattice antiferromagnet $CuFeO_2$ under pulsed high magnetic fields are reported. This material exhibits a distorted triangular lattice structure below ~11 K to relieve partially the geometric frustration. We find stepwise changes in the lattice constants, associated with the magnetization changes parallel ($H^{\parallel}$) and perpendicular ($H^{\perp}$) to the trigonal c axis. The relative changes in the lattice constant b with $H^{\parallel}$ are reproduced by a calculation based on a model in which the number of bonds connecting two parallel spins along the b axis increases with increasing field and the lattice contracts to gain the ferromagnetic direct and antiferromagnetic superexchange energies. For $H^{\perp}$, we find a discontinuous change in b and c at ~24 T, and a plateau in b and c at $24<H^{\perp}<30$ T. The change in b with increasing $H^{\perp}$ agrees also with the same calculation. We discuss the anisotropic behavior in $CuFeO_2$ observed at the low fields and find that the anisotropy is closely correlated with the lattice distortion.

DOI: 10.1103/PhysRevB.75.224411 PACS number(s): 75.25.+z, 75.80.+q, 75.50.Ee

I. INTRODUCTION

In many magnetic materials, the crystal lattice is coupled with the magnetic moments through magnetoelastic interaction. Typical examples are magnetostriction[1] and spin-Peierls transition.[2] In recent years, magnetic materials with geometric spin frustration, such as triangular and pyrochlore lattice antiferromagnets, have been attracting much attention, in which the magnetoelastic interaction also plays an important role. When the nearest-neighbor exchange interaction between magnetic moments on a tetrahedron of the pyrochlore lattice is antiferromagnetic, strong geometric frustration results. For classical spins, there are infinite ways of arranging spins on the vertices of a tetrahedron[3] with total spin $S_{\mathrm{tot}}=0$. Due to this vast degeneracy, a classical Heisenberg antiferromagnet on the pyrochlore lattice is predicted to be disordered down to absolute zero temperature.[4] In real pyrochlore magnets, however, a magnetic order has been observed at a finite temperature by breaking lattice symmetry.[5–9] Theory predicts that a Heisenberg antiferromagnet on the triangular lattice will show a noncollinear magnetic structure.[10] On the contrary, in $CuFeO_2$, which is an archetype triangular lattice antiferromagnet (TLA), a collinear magnetic structure has been observed.[11,12] The interrelation between the magnetic properties and the magnetoelastic interaction in $CuFeO_2$ is the subject of this paper.

The magnetic properties of $CuFeO_2$ have been studied extensively in the past 15 years.[11–29] $CuFeO_2$ has the delafossite structure, which belongs to the rhombohedral (trigonal) space-group $R\bar{3}m$ at room temperature and the lattice constants are $a=3.03$ Å and $c=17.17$ Å in the trigonal notation. The crystal consists of magnetic Fe^{3+}, nonmagnetic Cu^{1+}, and O^{2-} triangular lattice layers, which are stacked along the c axis. Since each Fe^{3+} layer is well separated by one Cu^{1+} and two O^{2-} layers, $CuFeO_2$ offers an excellent arena for the study of antiferromagnetism on the triangular lattice. Recently, Kimura *et al.*[30] have reported magnetic-field-induced ferroelectricity in $CuFeO_2$. This material is, therefore, a multiferroic where the inversion symmetry is broken by the magnetic ordering.

The magnetic ion Fe^{3+} in $CuFeO_2$ has the orbital singlet electronic configuration of ^6S (total spin $S=5/2$ and total orbital angular momentum $L=0$). Thus, the material is expected to be Heisenberg spin TLA, and its ground state should have the noncollinear three-sublattice 120° structure as described above. In contrast, a magnetic transition occurs at $T_{N2}\sim 11$ K to a collinear four-sublattice (4SL) $\uparrow\uparrow\downarrow\downarrow$ phase with the magnetic moments along the c axis. Between T_{N2} and $T_{N1}\sim 14$ K, a partially disordered phase exists whose magnetic structure is a sinusoidally modulated one with the moments along the c axis.[11,12,17,28]

Recently, Terada *et al.*[31] and Ye *et al.*[32] have reported a lattice distortion associated with the magnetic ordering from their x-ray-diffraction study. Moreover, Terada *et al.*[31] observed superlattice reflections below T_{N2} from which they proposed a "scalene triangle" (ST) lattice distortion shown in Fig. 1(a). The ST lattice distortion lifts the ground-state degeneracy of the TLA and leads to the 4SL ordering.

An interesting phenomenon has been found when $CuFeO_2$ is placed in a magnetic field. Ajiro *et al.*[14,15] have first measured the magnetization M in an applied magnetic field H. When H is applied along the c axis ($H^{\parallel}$) below T_{N2}, $CuFeO_2$ exhibits successive magnetization changes at $H^{\parallel}_{c1}\sim 7$ T, $H^{\parallel}_{c2}\sim 13$ T, $H^{\parallel}_{c3}\sim 20$ T, $H^{\parallel}_{c4}\sim 34$ T, and $H^{\parallel}_{c5}\sim 70$ T. In the neutron-diffraction measurements, reported by Petrenko *et al.*[22] and Mitsuda *et al.*,[21] the spin structures at $H^{\parallel}_{c1}\leqslant H^{\parallel}\leqslant H^{\parallel}_{c2}$ and $H^{\parallel}_{c2}\leqslant H^{\parallel}\leqslant H^{\parallel}_{c3}$ are determined to be an incommensurate one and collinear five-sublattice (5SL) $\uparrow\uparrow\uparrow\downarrow\downarrow$ one,

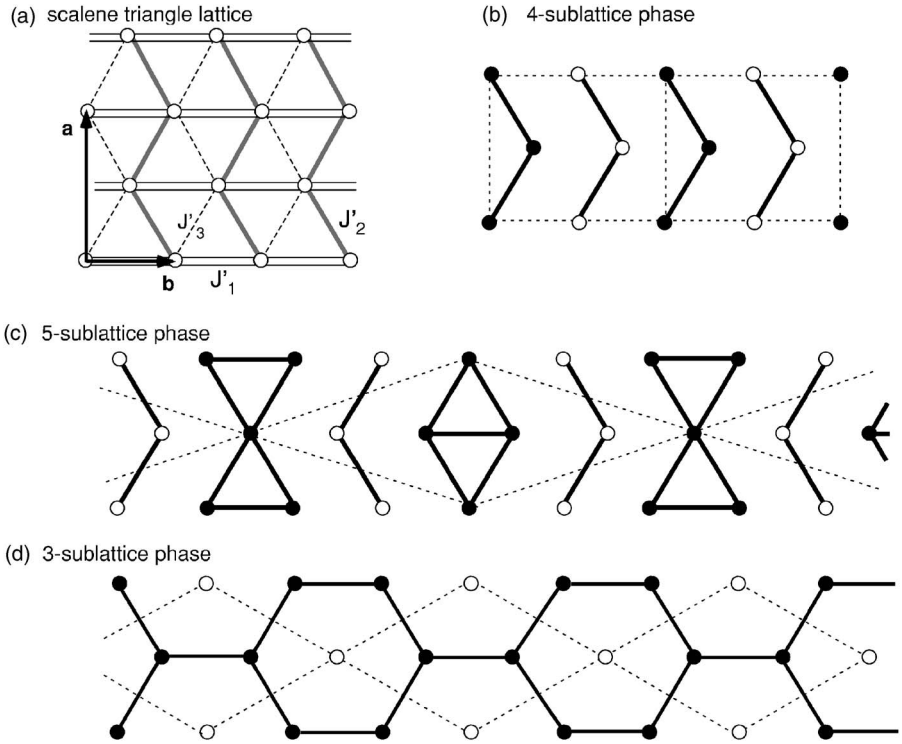

FIG. 1. Schematic drawings of (a) scalene triangular lattice, (b) four-sublattice (4SL) magnetic structure, (c) five-sublattice (5SL) magnetic structure, and (d) three-sublattice (3SL) magnetic structure in the basal plane with the respective unit cells drawn by the dotted lines. [(b)–(d)] Filled and empty circles denote up and down spins, respectively. The solid lines denote bonds connected by parallel spins.

respectively. Terada *et al.*[33] have revealed that the ST lattice distortion is relieved at $H_{c2}^{\parallel}$ and the crystal lattice changes to an "isosceles triangle" lattice from the observation of a disappearance of the superlattice reflection. The spin structures in the higher magnetic-field phases at $H_{c3}^{\parallel} \leqslant H^{\parallel} \leqslant H_{c4}^{\parallel}$ and $H_{c4}^{\parallel} \leqslant H^{\parallel} \leqslant H_{c5}^{\parallel}$ have not been determined experimentally.

When $CuFeO_2$ is placed in a magnetic field perpendicular to the c axis ($H^{\perp}$), a magnetization change has been found at $H^{\perp} \sim 24$ T.[15] Petrenko *et al.*[22] have shown that the 4SL magnetic structure remains unchanged up to $H^{\perp} = 14.5$ T in their neutron-diffraction measurements. Despite the orbital singlet state of Fe^{3+}, $CuFeO_2$ is found to show an anisotropic behavior depending on field orientations and field strengths as described above. This unconventional behavior has not been clarified.

We have reported the results of x-ray-diffraction measurements under pulsed high magnetic field parallel to the c axis of $CuFeO_2$.[34] The measurements have shown that the lattice constant b contracts stepwise with increasing $H^{\parallel}$ in coincidence with the multistep magnetization changes. In this paper, we report details of the synchrotron x-ray-diffraction measurements under pulsed high magnetic fields parallel as well as perpendicular to the c axis up to 38 T.

II. EXPERIMENTAL DETAILS

A single crystal of $CuFeO_2$, grown by the floating-zone technique[35] at RIKEN, was cut into a parallelepiped with dimensions $2 \times 2 \times 5$ mm^3. The samples used in the measurements for $H^{\parallel}$ and $H^{\perp}$ were cut from the same boule. Synchrotron x-ray-diffraction measurements in pulsed high magnetic fields were carried out at the beamline BL19LXU (Ref. 36) at SPring-8. This beamline is equipped with a 27 m undulator[37] and the world's strongest x rays are available.

We have made a new magnet (No. 4 magnet)[38] which has a larger inductance compared with the previous ones.[39] Figure 2 shows a schematic cross section of the split-pair magnet. The magnet has ~150 mm diameter and ~150 mm axial length and consists of 18 layers of coils wound with a Cu-Ag wire. Between the eighth and ninth layers, a space is provided to introduce liquid nitrogen for rapid cooling the interior of the magnet. In combination with a capacitor bank

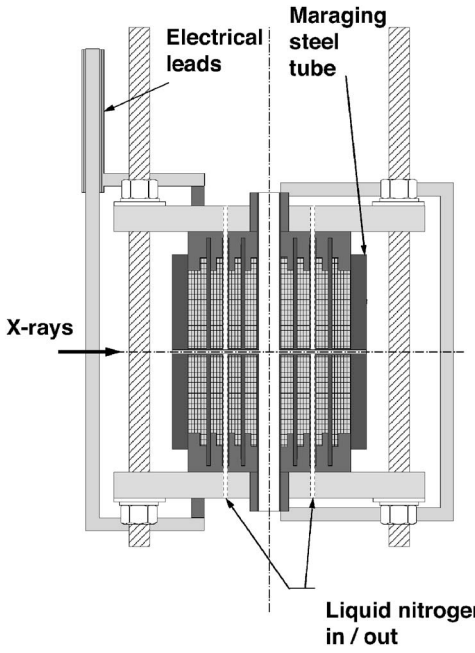

FIG. 2. Cross section of the No. 4 pulsed field magnet for the x-ray-diffraction measurement.

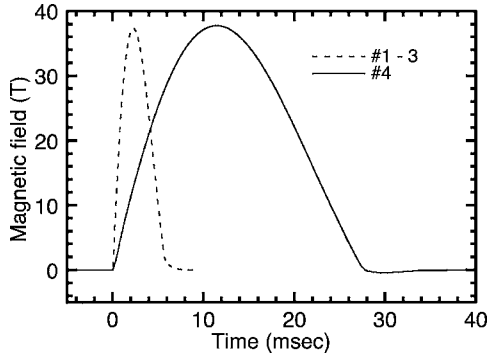

FIG. 3. Time variation of the pulsed magnetic field measured in the No. 4 magnet (full line) and that in the previous magnets (dotted line).

of 10 mF and 500 kJ, the pulse duration is increased to 27 ms, as shown in Fig. 3. These improvements make a precise measurement of field-induced phase transitions possible, because the change in magnetic field can be smaller for a given time window of the measurement. A glass Dewar can be inserted into the magnet and the sample temperature can be lowered to liquid-helium temperatures. The sample was mounted on a quartz rod and was inserted into the glass Dewar. The data were taken with a PILATUS 100 K detector system,[40] which is a single photon counting detector developed at the Paul Scherrer Institute, Switzerland.

In this paper, we conveniently use the two notations, trigonal and orthorhombic, to represent indices, while the actual crystal lattice symmetry in the low-temperature phase in $CuFeO_2$ is monoclinic.[32,33] The relation between the lattice constants in the trigonal cell (a_t, b_t, c_t) and the orthorhombic cell (a, b, c) is $a=\sqrt{3}a_t$, $b=b_t$ [see Fig. 1(a)], and $c=c_t$. The subscript t in the indices denotes the trigonal notation, and no indices are for the orthorhombic notation. We have performed measurements for two field orientations. One is, a vertical pulsed magnetic field is applied parallel to the c axis with the horizontal $(HK0)$ scattering plane. In this setup, we can measure the lattice constants a and b only. The other is, H is applied parallel to the a axis with the horizontal $(0KL)$ scattering plane. In this setup, we measure the lattice constants b and c. In addition, the lattice constant a can be measured owing to the monoclinic distortion. The sample was aligned to the magnetic field within ±0.5°.

The magnetization measurement for $H \| c$ was performed at KYOKUGEN, Osaka University and that for $H \perp c$ was done at ISSP, University of Tokyo, under pulsed high magnetic fields. The samples used in these magnetization measurements were cut from the same boule from which the samples used in the x-ray measurements were cut.

III. RESULTS

A. Magnetization measurements

1. Magnetic field parallel to the c axis: $H^{\|}$

Figure 4(a) shows the magnetization curve for $H^{\|}$ up to 40 T. With increasing $H^{\|}$, magnetization changes are observed at $H^{\|}_{c1} \sim 7$ T, $H^{\|}_{c2} \sim 13$ T, $H^{\|}_{c3} \sim 20$ T, and $H^{\|}_{c4} \sim 34$ T. The phases between the respective transition fields are labeled as $I_{\|}$, $II_{\|}$, $III_{\|}$, $IV_{\|}$, and $V_{\|}$. The transitions at the lower three critical fields, $H^{\|}_{c1}$, $H^{\|}_{c2}$, and $H^{\|}_{c3}$, are accompanied by a hysteresis indicating that these transitions are of first order. In phase $II_{\|}$, a linear increase in M with $H^{\|}$ is observed, indicating that the spin orientation continuously changes with $H^{\|}$, as reported before.[24,27] In phase $III_{\|}$, M is almost independent of $H^{\|}$ and the magnitude is about one-fifth of the saturation value, $5\mu_B/Fe^{3+}$, where μ_B is the Bohr magneton. This is consistent with the 5SL magnetic structure (↑↑↑↓↓) (Refs. 21 and 22) shown in Fig. 1(c).

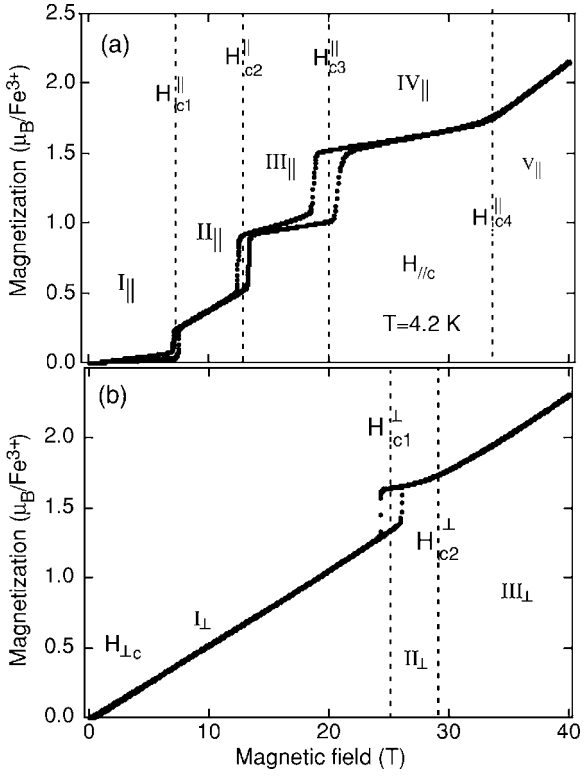

FIG. 4. Magnetic-field dependence of the magnetization in $CuFeO_2$ (a) parallel and (b) perpendicular to the c axis, respectively.

In phase $IV_{\|}$, M is almost independent of $H^{\|}$ and the magnitude is almost one-third of the saturation value. The magnetic structure in phase $IV_{\|}$ has not been determined experimentally. From the one-third magnetization, one may assume a collinear three-sublattice (3SL) magnetic structure (↑↑↓) shown in Fig. 1(d). With further increase in $H^{\|}$, M starts to increase again at $H^{\|}_{c4}$. $dM/dH^{\|}$ in phase $V_{\|}$ is almost equal to that in phase $II_{\|}$. Since no discontinuous change is observed at $H^{\|}_{c4}$ in the magnetization curve, spins in the 3SL structure start to change their directions gradually toward $\vec{H}$ above $H^{\|}_{c4}$, which may be called a canted 3SL structure.

We comment on the thermal equilibrium in our pulsed field measurements. As stated above, the transitions at the lower three critical fields, $H^{\|}_{c1}$, $H^{\|}_{c2}$, and $H^{\|}_{c3}$, are accompanied by a hysteresis. On the contrary, the magnetizations measured in increasing and decreasing fields are identical in phases $I_{\|}$, $II_{\|}$, $IV_{\|}$, and $V_{\|}$, except in the vicinity of the critical fields. We have also measured the magnetization with differ-

ent field sweep rates and did not find any detectable change. We, therefore, conclude that the sample is in thermal equilibrium at phases $I_{\parallel}$, $II_{\parallel}$, $IV_{\parallel}$, and $V_{\parallel}$ during sweeping magnetic fields.

2. Magnetic field perpendicular to the c axis: $H^{\perp}$

Figure 4(b) shows the magnetization curve for $H^{\perp}$. With increasing $H^{\perp}$, a linear increase in M is observed at $0 \leqslant H^{\perp} \leqslant H_{c1}^{\perp} \sim 24$ T. In the previous neutron-diffraction measurements under $H^{\perp}$, the 4SL magnetic structure has been reported to remain unchanged up to $H^{\perp}=14.5$ T.[22] Since there exists a finite uniform magnetization perpendicular to the c axis for nonzero $H^{\perp}$, spins in the 4SL $\uparrow\uparrow\downarrow\downarrow$ magnetic structure with the easy axis along c gradually change their direction toward the basal plane in phase $I_{\perp}$. A discontinuous change in M is seen at $H_{c1}^{\perp} \sim 24$ T, which is consistent with the previous measurements.[14] This magnetization change is associated with a hysteresis indicating that the phase transition is of first order.

The magnetization is almost independent of magnetic field at $H_{c1}^{\perp} \leqslant H^{\perp} \leqslant H_{c2}^{\perp} \sim 30$ T and the magnitude of which is about one-third of the saturation moment. This result suggests that a spin rearrangement occurs at $H_{c1}^{\perp}$ from the canted 4SL structure with the easy axis parallel to c to the 3SL structure with the moments in the basal plane. With further increase in $H^{\perp}$, M starts to increase again at $H_{c2}^{\perp}$. This means that spins start to change their direction from $\vec{H}^{\perp}$. This behavior in the magnetization curve in phases $II_{\perp}$ and $III_{\perp}$ is the same as that in phases $IV_{\parallel}$ and $V_{\parallel}$, except the spin orientations and the critical fields.

As is seen in Fig. 4, while the magnetization process is anisotropic below ~24 T, it becomes isotropic above ~24 T. As mentioned in the Introduction, one of the puzzling problems to be solved in the magnetic properties of $CuFeO_2$ is the anisotropic behavior, despite the orbital singlet state of the Fe^{3+} ion. From the present experiment, we find that the anisotropic behavior seen at the low-field region disappears above ~24 T. The magnetization process measured previously on a powder sample[14] shows a plateaulike behavior at ~24 T and an increase in M above 24 T, in which dM/dH is almost the same as that observed in the single-crystal measurements.

B. X-ray-diffraction measurements

1. Magnetic field parallel to the c axis: $H^{\parallel}$

Figure 5 shows images of the diffraction pattern around the $(110)_t$ Bragg point. As is seen in Figs. 5(a) and 5(b), a single peak at $(110)_t$ observed at 38 K splits into two peaks at 4.2 K. This indicates that the trigonal threefold rotational symmetry along the c axis is broken at 4.2 K, which corresponds to a change in lattice symmetry from trigonal to monoclinic.[32,33] This result is consistent with the previous x-ray measurements.[31–33] As is seen in Fig. 5(c), the distance between the two peaks is significantly reduced at $H^{\parallel}=32.3$ T. The splitting in the peaks at 32.3 T indicates that the crystal lattice symmetry remains monoclinic even in phase $IV_{\parallel}$.

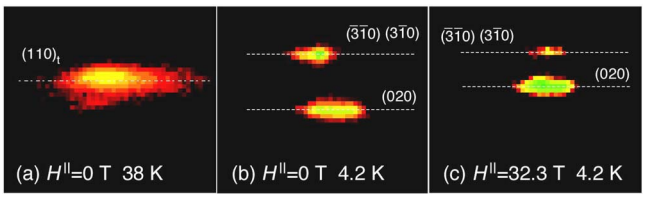

FIG. 5. (Color online) X-ray-diffraction images around the trigonal (110) reciprocal-lattice point, obtained (a) at $T=38$ K and $H^{\parallel}=0$ T, (b) $T=4.2$ K and $H^{\parallel}=0$ T, and (c) at $T=4.2$ K and $H^{\parallel}=32.3$ T. Vertical direction in these images corresponds to the scattering angle.

We deduce the lattice constants a and b from the peak positions at the (020) and $(3\bar{1}0)$ [or $(\bar{3}\bar{1}0)$] reflections. Figure 6 shows the $H^{\parallel}$ dependence of the lattice constants a and b obtained at $T=4.2$ K. We see that the lattice constant b contracts stepwise with increasing $H^{\parallel}$ in coincidence with the multistep magnetization changes. The result obtained at low fields, below ~15 T, is consistent with the previous x-ray-diffraction measurements under static magnetic fields[33] and with the macroscopic magnetostriction measurements.[30] The change in the lattice constant a is much smaller than that in b. We thus find that the lattice change along the b axis, not the a axis, is strongly correlated with the multistep magnetization changes. The changes in c are also correlated with the magnetization changes in $H^{\parallel}$, as reported in the magnetostriction measurements.[30] It is not possible to measure the lattice changes along the applied magnetic-field direction in the present setup. In the future, it will be possible to do this kind of measurement using a horizontal field pulsed magnet.

2. Magnetic field perpendicular to the c axis: $H^{\perp}$

We measured the magnetic-field dependence of the Bragg reflections around $(110)_t$ and $(009)_t$ reciprocal-lattice points, in order to investigate the lattice changes both in the basal plane and along the c axis. Typical x-ray-diffraction images are displayed in Fig. 7. In zero magnetic field and at 4.2 K, Bragg reflections assigned as (020), $(3\bar{1}0)$ [or $(\bar{3}\bar{1}0)$], and (009) are observed [see Figs. 7(a) and 7(d)]. This result is consistent with that observed in the different setup shown in

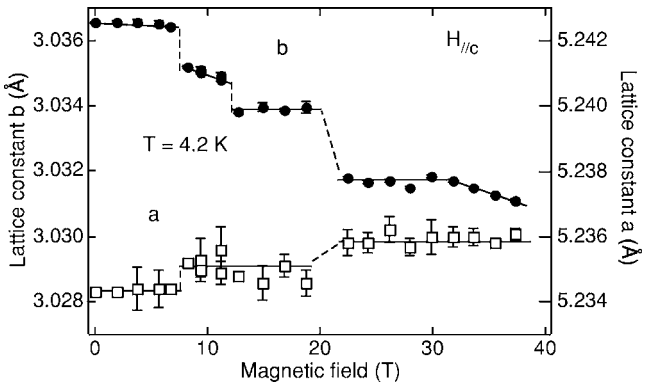

FIG. 6. Magnetic-field dependence of the lattice constants a (squares) and b (circles) at $T=4.2$ K. The magnetic field is applied along the c axis.

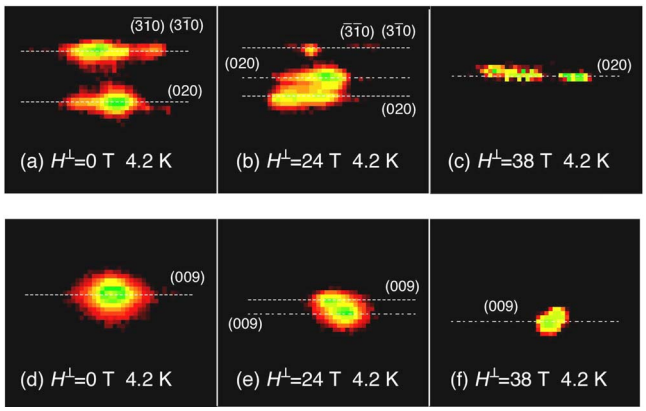

FIG. 7. (Color online) X-ray-diffraction images around [(a)–(c)] the trigonal (110) and [(d)–(f)] the (009) reciprocal-lattice points, obtained at T=4.2 K. [(a) and (d)] $H^{\perp}$=0 T, [(b) and (e)] $H^{\perp}$=24 T, and [(c) and (f)] $H^{\perp}$=38 T. Vertical direction in these images corresponds to the scattering angle.

Fig. 5(b) and is also consistent with the previous measurements in zero field.[31]

Only a single peak is observed at 38 T, as shown in Fig. 7(c). At an intermediate field, this peak coexists with the two peaks observed in zero field, as shown in Fig. 7(b). We propose the following two possibilities for the appearance of the new (020) reflection observed at $H^{\perp}$=24 and 38 T. One is that a first-order phase transition from a monoclinic to a second monoclinic structures occurs. In the high-field monoclinic phase above $H_{c1}^{\perp}$, a single domain state is considered to be realized with the application of H along the a axis. The other possibility is that a first-order structural phase transition from monoclinic to trigonal occurs. Considering the experimental result that the crystal symmetry in phase $IV_{\parallel}$ remains monoclinic, we conclude that the former possibility is probable.

As shown in Figs. 7(e) and 7(f), a new Bragg reflection assigned as (009) appears above $H_{c1}^{\perp}$. This (009) reflection coexists at $H_{c1}^{\perp}$ with the (009) reflection observed in zero field and the new (009) reflection remains above $H_{c1}^{\perp}$. These results imply that a first- order structural phase transition occurs at $H_{c1}^{\perp}$.

Figure 8 shows the $H^{\perp}$ dependence of the lattice constants a, b, and c obtained from the present experiment. In phase $I_{\perp}$ where the canted 4SL state is realized, the lattice constant a elongates, b contracts, and c elongates with increasing $H^{\perp}$. The lattice constant c increases as H^2 up to $H_{c1}^{\perp}$. This quadratic dependence of lattice constants on H originates from an exchange striction, as observed in CoO.[41] The lattice constants change discontinuously at $H_{c1}^{\perp}$. In phase $II_{\perp}$, b and c are independent of $H^{\perp}$. This *plateau* in the field dependence of the lattice constants nicely corresponds to the magnetization plateau with one-third of the saturation value [Fig. 4(b)]. Note that the value of b in $II_{\perp}$ is almost the same as that in $IV_{\parallel}$. This result provides an evidence that the magnetic structure in phase $II_{\perp}$ is the same as that in phase $IV_{\parallel}$ apart from the spin orientations. With further increase in $H^{\perp}$, the lattice constants start to change again at $H_{c2}^{\perp}$. Above $H_{c2}^{\perp}$, the change in b with increasing $H^{\perp}$ is almost the same as that in b with increasing $H^{\parallel}$ above $H_{c4}^{\parallel}$.

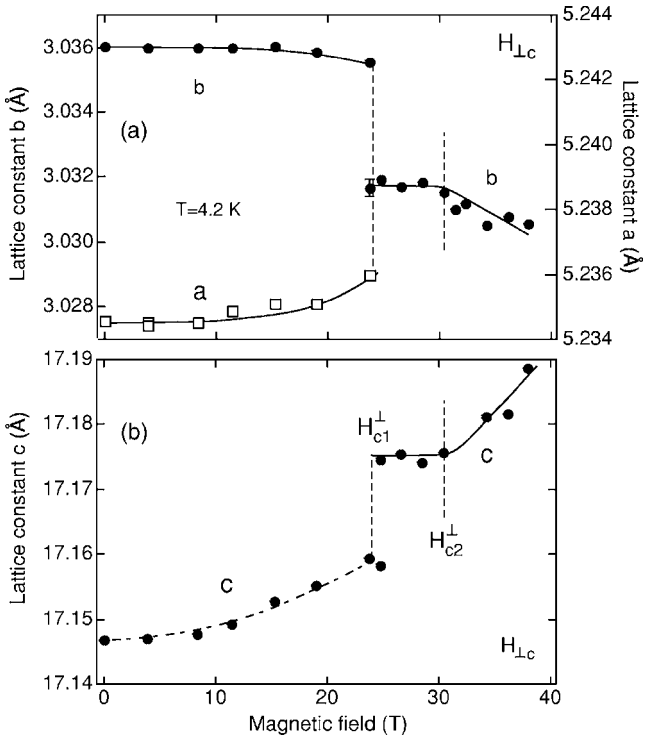

FIG. 8. Magnetic-field dependence of the lattice constants (a) a (squares), b (circles) and (b) c (circles) at T=4.2 K. The magnetic field is applied along the a axis. Solid lines are drawn as a guide for the eyes. Dash-dotted line shows a quadratic fit to the data as discussed in the text.

IV. DISCUSSION

A. Stepwise lattice changes

We discuss the stepwise changes in the lattice constant b. As mentioned in the Introduction, the 4SL ↑↑↓↓ state is realized in zero magnetic field accompanied by the scalene triangle lattice distortion shown in Fig. 1(a).[31] For the origin of the magnetoelastic coupling, we invoke the exchange interactions among Fe^{3+} spins and their distance dependence. As was discussed by Mekata *et al.*,[12] the nearest-neighbor exchange interaction in the basal plane of $CuFeO_2$ is a sum of the direct exchange interaction, which is assumed to be ferromagnetic, and the 90° superexchange interaction through an O^{2-} ion. The superexchange interaction between $3d^5$ spins involves several mechanisms and the sign is uncertain.[42] Kanamori suggested that the 90° superexchange interaction between spins in the $3d^5$ system would be antiferromagnetic,[42] and we believe that this is the case judging from the antiferromagnetic ordering in this compound. The experimental evidence that the b axis elongates at low temperatures in zero field implies that the direct exchange interaction diminishes and the antiferromagnetic interaction dominates. In the following, we consider only the nearest-neighbor interactions along the three edges of a triangle and further neighbor interactions introduced in the previous studies[12,17] are neglected. Figure 1(b) represents the 4SL state in the basal plane determined from the neutron-diffraction studies.[11,12,32] In the 4SL state, all spins connected by the nearest-neighbor J_1' bonds along the b axis are anti-

ferromagnetically aligned, and the spin arrangement in the J_1' row is $\uparrow\downarrow\uparrow\downarrow$. In phase $II_{\parallel}$, noncollinear magnetic structure is realized as has been determined in the recent neutron-diffraction study.[43] In the 5SL $\uparrow\uparrow\uparrow\downarrow\downarrow$ state in phase $III_{\parallel}$, one of the five bonds along the J_1' row in the unit cell accommodates two parallel spins at the ends as shown by the horizontal solid line in Fig. 1(c) and costs excess energy. In order to lower this excess in the exchange energy, the lattice constant b contracts to resume the ferromagnetic direct exchange interaction. This lattice contraction also gains the antiferromagnetic superexchange energy because the bond angle Fe-O-Fe becomes close to 90°. The 180° superexchange interaction between Fe^{3+} spins is predicted to be antiferromagnetic.[42] Similarly, in the 3SL $\uparrow\uparrow\downarrow$ state in phase $IV_{\parallel}$, one of the three bonds along the J_1' row in the unit cell accommodates two parallel spins at the ends, as shown by horizontal solid lines in Fig. 1(d). Therefore, an additional lattice contraction along b is needed.

We calculate the change in the lattice constant b in applied magnetic fields. Writing the undistorted bond length along b as d, the bond length elongates to $d+\delta$ ($\delta>0$) when two antiparallel spins are connected by this bond to gain the ferromagnetic direct and antiferromagnetic superexchange energies. Similarly, the bond length contracts to $d-\delta$ when two parallel spins are connected by this bond. The calculated bond lengths averaged over the unit cells in the 4SL (d_{4SL}), 5SL (d_{5SL}), and 3SL (d_{3SL}), the saturated ferromagnetic (d_{FM}), and the paramagnetic (PM) phases (d_{PM}) are

$$d_{4SL} = d + \delta, \tag{1}$$

$$d_{5SL} = d + (3/5)\delta, \tag{2}$$

$$d_{3SL} = d + (1/3)\delta, \tag{3}$$

$$d_{FM} = d - \delta, \tag{4}$$

and

$$d_{PM} = d. \tag{5}$$

The changes in the bond length Δd from the 4SL phase are given as

$$\Delta d_{5SL} = d_{5SL} - d_{4SL} = -(2/5)\delta, \tag{6}$$

$$\Delta d_{3SL} = d_{3SL} - d_{4SL} = -(2/3)\delta, \tag{7}$$

$$\Delta d_{FM} = d_{FM} - d_{4SL} = -2\delta, \tag{8}$$

and

$$\Delta d_{PM} = d_{PM} - d_{4SL} = -\delta. \tag{9}$$

The changes in the lattice parameter in respective phase relative to that in the FM phase, $\Delta d_m' \equiv \Delta d_m / \Delta d_{FM}$ (m=4SL, 5SL, 3SL, and PM), are

$$\Delta d_{4SL}' = 0, \tag{10}$$

$$\Delta d_{5SL}' = 1/5, \tag{11}$$

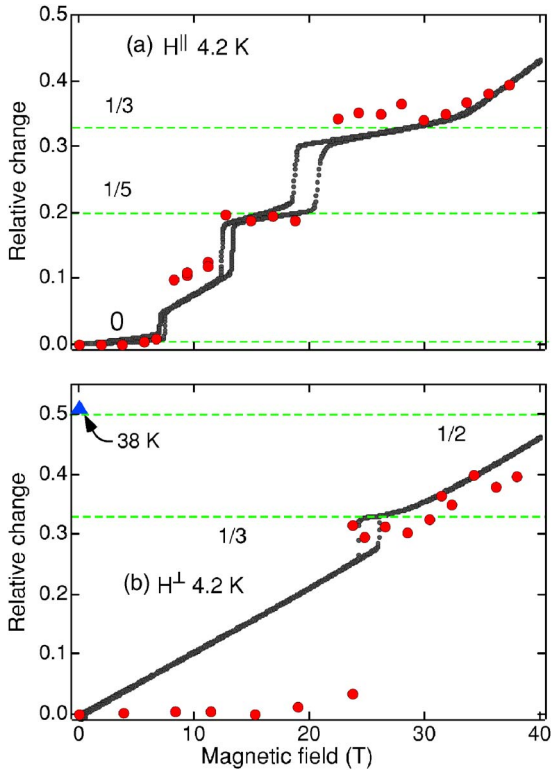

FIG. 9. (Color online) (a) $H^{\parallel}$ and (b) $H^{\perp}$ dependence of relative changes of the magnetization normalized with the saturation moment $5\mu_B/Fe^{3+}$ and the relative change in the lattice constant, $\alpha[b(H^{\parallel}=0\ \mathrm{T})-b(H^{\parallel})]/b(H^{\parallel}=0\ \mathrm{T})$, where α is a numerical factor. Circles and triangle denote relative changes in the lattice constant measured at 4.2 and 38 K, respectively. Dots denote relative changes in the magnetizations.

$$\Delta d_{3SL}' = 1/3, \tag{12}$$

and

$$\Delta d_{PM}' = 1/2. \tag{13}$$

We plot in Fig. 9(a) the relative change in the lattice constant b as a function of $H^{\parallel}$ together with the magnetization curve. We see that the two quantities are nicely correlated. The dotted lines in Fig. 9(a) represent Eqs. (10)–(12) and we see a good agreement with our observation. The changes in b with application of $H^{\perp}$ are calculated similarly and the result shows that they occur at 1/3 and 1/2, as shown in Fig. 9(b).

B. Anisotropic behavior in $CuFeO_2$

We discuss the anisotropic behavior of $CuFeO_2$. As mentioned in the Introduction, since Fe^{3+} has the orbital singlet electronic configuration ^6S, the magnetic properties in $CuFeO_2$ are expected to be isotropic. Nevertheless, the magnetic properties below $T_{N1} \sim 14$ K are anisotropic, as observed by a lot of macroscopic and microscopic measurements.[11,12,14,15,17,19–24,26–29] The present magnetization measurements show that while the magnetization curve is different for $H \| c$ and $H \perp c$ below ~24 T, it becomes almost identical above ~24 T. Moreover, the present x-ray-

diffraction measurements show that the changes in the lattice constant b with increasing $H^{\parallel}$ and $H^{\perp}$ are almost identical above ~24 T, despite the large difference below 24 T. These experimental results suggest that the anisotropic magnetism of $CuFeO_2$ is closely correlated with the lattice distortion.

Fukuda *et al.*[18] have done an electron-spin-resonance (ESR) measurement on $CuFeO_2$. They observed several ESR branches in phases $I_{\parallel}$, $II_{\parallel}$, $III_{\parallel}$, and $IV_{\parallel}$ when H is applied parallel to c at $T=1.7$ K. From the slope of the lines drawn through the data points in the frequency-field plot,[18] we estimate $g_{I_{\parallel}} \simeq 1.6$ and $g_{III_{\parallel}} \simeq 1.8-1.9$ in phases $I_{\parallel}$ and $III_{\parallel}$, respectively. In phase $IV_{\parallel}$, the higher- (h) and lower (l)-frequency branches give $g^h_{IV_{\parallel}} \simeq 2.0$ and $g^l_{IV_{\parallel}} \simeq 1.7$, respectively. The difference in the g values between the h and l branches is not understood at this stage. Further ESR studies will clarify this point. From the ESR measurement, the g value is seen to increase with increasing field and finally becomes $\simeq 2.0$, i.e., becomes isotropic above $H^{\parallel}_{c3}$. This result is consistent with the present magnetization and x-ray-diffraction measurements.

We discuss briefly a possible origin of the g shift. The orbital momentum should vanish in the $3d^5$ half-filled Fe^{3+} ions under cubic crystalline field, which remains unchanged under a crystalline field with lower symmetry. The isotropic ionic orbital states generally lead to isotropic bonding with oxygen ions and the g value should be 2.00. However, as was previously reported in another $3d^5$ system $GaFeO_3$,[44] if the Fe^{3+} deviates from the center position of the oxygen octahedron, the deviation might induce an anisotropy in the Fe $3d$-O $2p$ hybridization and the O $2p$ to Fe $3d$ charge transfer. The g shift is given by

$$2 - 2\lambda \sum_{e} (\langle g|L_{\mu}|e\rangle\langle e|L_{\nu}|g\rangle)/(E_e - E_g), \qquad (14)$$

where λ is the spin-orbit interaction constant, E_g and E_e are the energies of the ground and excited states, respectively, and L_{μ} and L_{ν} are the μ and ν ($\mu, \nu = x, y, z$) components of the orbital momentum L, respectively. To make the g value smaller than 2, λ should be positive. This means that the number of $3d$ electrons at the Fe site should be less than 5, suggesting that an Fe^{4+} state is mixed. At higher fields, the lattice becomes isotropic and the hybridization and charge transfer become isotropic giving $g \simeq 2$. The same calculation produces a single-ion anisotropy, DS_z^2. Petrenko *et al.* assumed the presence of a single-ion anisotropy to discuss the magnetic properties of $CuFeO_2$.[27] For further investigation of the origin of the anisotropic magnetoelastic interaction in $CuFeO_2$, the measurements that can directly probe the electronic states of Fe^{3+} and O^{2-}, such as x-ray-absorption spectroscopy, x-ray magnetic circular dichroism, x-ray photoemission spectroscopy, and ^{17}O nuclear-magnetic-resonance spectroscopy, are required.

Using the value $g=1.6$ in the 4SL phase, we obtain the magnetic moment given by $g\mu_B S = 4.0\mu_B$/Fe in agreement with that obtained from neutron-diffraction measurements.[11,12,32] The value $5\mu_B$/Fe would be expected from $g=2.0$.

V. CONCLUSIONS

We have performed synchrotron x-ray-diffraction and magnetization measurements on a triangular lattice antiferromagnet $CuFeO_2$ under pulsed high magnetic fields up to 40 T. With increasing $H^{\parallel}$, the orthorhombic lattice constant b changes stepwise at $H^{\parallel}_{c1} \sim 7$ T, $H^{\parallel}_{c2} \sim 13$ T, $H^{\parallel}_{c3} \sim 20$ T, and $H^{\parallel}_{c4} \sim 34$ T, in coincidence with the multistep magnetization changes. The relative changes in b are scaled with the magnetization changes. We find that the changes in b with application of $H^{\parallel}$ are reproduced by our calculation based on a simple model in which the number of bonds connecting two parallel spins along the b axis increases with the change in the magnetic structure under an applied magnetic field, and b contracts to gain the direct ferromagnetic and antiferromagnetic superexchange energies. For $H^{\perp}$, we find a discontinuous change in orthorhombic b and c at $H^{\perp}_{c1} \sim 24$ T and a plateau in the field dependence of b and c at $H^{\perp}_{c1} < H^{\perp} < H^{\perp}_{c2} \sim 30$ T. The structural phase-transition field coincides with the critical field observed in the magnetization measurement along $H^{\perp}$. The change in b with increasing $H^{\perp}$ is also reproduced by our calculation.

We have discussed the anisotropic behavior in $CuFeO_2$ observed at the low fields. We find that the anisotropy is closely correlated with the lattice distortion.

ACKNOWLEDGMENTS

N.T. was supported by the Special Researchers' Basic Science Program (RIKEN). This work was supported in part by a Grant-in-Aid for Scientific Research on Priority Areas "High Field Spin Science in 100 T" (No. 451) from the Ministry of Education, Culture, Sports, Science and Technology (MEXT) and by a Grant-in-Aid for Scientific Research from the Japan Society for the Promotion of Science.

*Present address: National Institute for Materials Science, 1-1, Namiki, Tsukuba, Ibaraki 305-0044, Japan.

[1] For a review, see J. Kanamori, *Magnetism*, edited by G. T. Rado and H. Suhl (Academic, New York, 1963), Vol. I, p. 127.

[2] For a review, see J. W. Bray, L. V. Interrante, I. S. Jacobs, and J. C. Bonner, *Extended Linear Chain Compounds*, edited by J. S. Miller (Plenum, New York, 1983), Vol. 3, p. 353.

[3] P. W. Anderson, Phys. Rev. **102**, 1008 (1956).

[4] R. Moessner and J. T. Chalker, Phys. Rev. Lett. **80**, 2929 (1998).

[5] Y. Yamashita and K. Ueda, Phys. Rev. Lett. **85**, 4960 (2000).

[6] O. Tchernyshyov, R. Moessner, and S. L. Sondhi, Phys. Rev. Lett. **88**, 067203 (2002).

[7] S. H. Lee, C. Broholm, T. H. Kim, W. Ratcliff II, and S. W. Cheong, Phys. Rev. Lett. **84**, 3718 (2000).

[8] H. Ueda, H. A. Katori, H. Mitamura, T. Goto, and H. Takagi, Phys. Rev. Lett. **94**, 047202 (2004).

[9] H. Ueda, H. Mitamura, T. Goto, and Y. Ueda, Phys. Rev. B **73**, 094415 (2006).
[10] S. Miyashita, J. Phys. Soc. Jpn. **55**, 3605 (1986).
[11] S. Mitsuda, H. Yoshizawa, N. Yaguchi, and M. Mekata, J. Phys. Soc. Jpn. **60**, 1885 (1991).
[12] M. Mekata, N. Yaguchi, T. Takagi, T. Sugino, S. Mitsuda, H. Yoshizawa, N. Hosoito, and T. Shinjo, J. Phys. Soc. Jpn. **62**, 4474 (1993).
[13] K. Takeda, K. Miyake, M. Hitaka, T. Kawae, N. Yaguchi, and M. Mekata, J. Phys. Soc. Jpn. **63**, 2017 (1994).
[14] Y. Ajiro, T. Asano, T. Takagi, M. Mekata, H. Aruga Katori, and T. Goto, Physica B **201**, 71 (1994).
[15] Y. Ajiro, K. Hanasaki, T. Asano, T. Takagi, M. Mekata, H. Aruga Katori, and T. Goto, J. Phys. Soc. Jpn. **64**, 3643 (1995).
[16] T. Takagi and M. Mekata, J. Phys. Soc. Jpn. **64**, 4609 (1995).
[17] S. Mitsuda, N. Kasahara, T. Uno, and M. Mase, J. Phys. Soc. Jpn. **67**, 4026 (1998).
[18] T. Fukuda, H. Nojiri, M. Motokawa, T. Asano, M. Mekata, and Y. Ajiro, Physica B **246-247**, 569 (1998).
[19] S. Mitsuda, T. Uno, M. Mase, H. Nojiri, K. Takahashi, M. Motokawa, and M. Arai, J. Phys. Chem. Solids **60**, 1249 (1999).
[20] S. Mitsuda, M. Mase, T. Uno, H. Kitazawa, and H. Aruga Katori, J. Phys. Soc. Jpn. **69**, 33 (2000).
[21] S. Mitsuda, M. Mase, K. Prokes, H. Kitazawa, and H. Aruga Katori, J. Phys. Soc. Jpn. **69**, 3513 (2000).
[22] O. A. Petrenko, G. Balakrishnan, M. R. Lees, D. M. Paul, and A. Hoser, Phys. Rev. B **62**, 8983 (2000).
[23] M. Hasegawa, M. I. Batrashevich, T. R. Zhao, H. Takei, and T. Goto, Phys. Rev. B **63**, 184437 (2001).
[24] N. Terada, S. Mitsuda, K. Prokes, O. Suzuki, H. Kitazawa, and H. A. Katori, Phys. Rev. B **70**, 174412 (2004).
[25] W. M. Xu, M. P. Pasternak, and R. D. Taylor, Phys. Rev. B **69**, 052401 (2004).
[26] N. Terada, S. Mitsuda, Y. Oohara, H. Yoshizawa, and H. Takei, J. Magn. Magn. Mater. **272-276S**, E997 (2004).
[27] O. A. Petrenko, M. R. Lee, G. Balakrishnan, S. de Brion, and G. Chouteau, J. Phys.: Condens. Matter **17**, 2741 (2005).
[28] N. Terada, T. Kawasaki, S. Mitsuda, H. Kimura, and Y. Noda, J. Phys. Soc. Jpn. **74**, 1561 (2005).
[29] N. Terada, S. Mitsuda, T. Fujii, and D. Petitgrand, J. Phys.: Condens. Matter **19**, 145241 (2007).
[30] T. Kimura, J. C. Lashley, and A. P. Ramirez, Phys. Rev. B **73**, 220401(R) (2006).
[31] N. Terada, S. Mitsuda, H. Ohsumi, and K. Tajima, J. Phys. Soc. Jpn. **75**, 023602 (2006).
[32] F. Ye, Y. Ren, Q. Huang, J. A. Fernandez-Baca, Pengcheng Dai, J. W. Lynn, and T. Kimura, Phys. Rev. B **73**, 220404(R) (2006).
[33] N. Terada, Y. Tanaka, Y. Tabata, K. Katsumata, A. Kikkawa, and S. Mitsuda, J. Phys. Soc. Jpn. **75**, 113702 (2006).
[34] N. Terada, Y. Narumi, K. Katsumata, T. Yamamoto, U. Staub, K. Kindo, M. Hagiwara, Y. Tanaka, A. Kikkawa, H. Toyokawa, T. Fukui, R. Kanmuri, T. Ishikawa, and H. Kitamura, Phys. Rev. B **74**, 180404(R) (2006).
[35] T. R. Zhao, M. Hasegawa, and H. Takei, J. Cryst. Growth **166**, 408 (1996).
[36] M. Yabashi, T. Mochizuki, H. Yamazaki, S. Goto, H. Ohashi, K. Takeshita, T. Ohata, T. Matsushita, K. Tamasaku, Y. Tanaka, and T. Ishikawa, Nucl. Instrum. Methods Phys. Res. A **467-468**, 678 (2001).
[37] T. Hara, M. Yabashi, T. Tanaka, T. Bizen, S. Goto, X. M. Marechal, T. Seike, K. Tamasaku, T. Ishikawa, and H. Kitamura, Rev. Sci. Instrum. **73**, 1125 (2002).
[38] Y. Narumi, K. Kindo, K. Katsumata, M. Kawauchi, Ch. Broennimann, U. Staub, H. Toyokawa, Y. Tanaka, A. Kikkawa, T. Yamamoto, M. Hagiwara, T. Ishikawa, and H. Kitamura, J. Phys.: Conf. Ser. **51**, 494 (2006).
[39] Y. Narumi, K. Kindo, K. Katsumata, M. Kawauchi, Ch. Broennimann, U. Staub, H. Toyokawa, Y. Tanaka, A. Kikkawa, T. Yamamoto, M. Hagiwara, T. Ishikawa, and H. Kitamura, J. Synchrotron Radiat. **13**, 271 (2006).
[40] Ch. Broennimann, E. F. Eikenberry, B. Henrich, R. Horisberger, G. Huelsen, E. Pohl, B. Schmitt, C. Schulze-Briese, M. Suzuki, T. Tomizaki, H. Toyokawa, and A. Wagner, J. Synchrotron Radiat. **13**, 120 (2006).
[41] Y. Narumi, K. Katsumata, U. Staub, K. Kindo, M. Kawauchi, Ch. Broennimann, H. Toyokawa, Y. Tanaka, A. Kikkawa, T. Yamamoto, M. Hagiwara, T. Ishikawa, and H. Kitamura, J. Phys. Soc. Jpn. **75**, 075001 (2006).
[42] J. Kanamori, J. Phys. Chem. Solids **10**, 87 (1959).
[43] T. Nakajima, S. Mitsuda, S. Kanetsuki, K. Prokes, A. Podlesnyak, H. Kimura, and Y. Noda, J. Phys. Soc. Jpn. **76**, 043709 (2007).
[44] J.-Y. Kim, T. Y. Koo, and J.-H. Park, Phys. Rev. Lett. **96**, 047205 (2006).